Influence of diapirs on the development of non-cylindrical arcuate fold-and-thrust belts: Results from analogue models of progressive arcs

Influencia de los diapiros en el desarrollo de cinturones de pliegues y cabalgamientos arqueados no cilíndricos: Resultados de modelos analógicos de arcos progresivos

Ana Crespo-Blanc[1], Alejandro Jiménez-Bonilla[2], Juan Carlos Balanyá[2], Inmaculada Expósito[2] y Manuel Díaz-Azpiroz[2]

[1] Departamento de Geodinámica – IACT, Universidad de Granada – CSIC, 18071. Granada, Spain. acrespo@ugr.es
[2] Departamento de Sistemas Físicos, Químicos y Naturales, Universidad Pablo de Olavide, C. Utrera, km. 1, Spain.
ajimbon@upo.es; jcbalrou@upo.es; iexpram@upo.es; mdiaazp@upo.es

ABSTRACT

In this paper, we present analogue models built to test the diapir role on the along-strike segmentation of fold-and-thrust belts in progressive arcs. To model the progressive arc, we used a protruding backstop that deformed in map view while the experiments run. This backstop indented a parallelepiped formed by silicone at the bottom and sand, in which silicone cylinders were added to simulate diapirs. Various types of models with different size and distribution of the diapirs were made in order to investigate the strain partitioning modes around these heterogeneities. The deformation style of the models is characterized by a highly non-cylindrical arcuate fold-and-thrust belt with blocks bounded by normal or strike-slip faults that strongly rotated clockwise or anticlockwise. The diapirs are key heterogeneities for the nucleation and linking of structures at the beginning of the experiment. When shortening proceed, their influence on the fold-and-thrust belt geometry diminished with respect to that of the backstop protrusion.

Key-words: *progressive arc, fold-and-thrust belt, diapir, analogue model.*

RESUMEN

En este artículo, se presentan modelos analógicos ideados para testar el papel de diapiros sobre el patrón estructural de cinturones de pliegues y cabalgamientos en arcos progresivos. Para modelizar el arco progresivo, se usa un backstop cuyo grado de protrusión aumenta progresivamente. El paralelepípedo inicial está formado por silicona y arena, con cilindros de silicona añadidos para simular los diapiros. Se hicieron varios modelos con distintos tamaños y distribución de diapiros, para indagar en el modo de partición de la deformación alrededor de estas heterogeneidades. El estilo de deformación de los modelos está caracterizado por cinturones de pliegues y cabalgamientos no cilíndricos, divididos en bloques por fallas normales y de salto en dirección, que rotan independientemente. Al principio del experimento, se nuclean las estructuras sobre los diapiros. Cuando aumenta el acortamiento, su influencia disminuye con respecto a la protrusión del arco.

Palabras clave: *arco progresivo, cinturón de pliegues y cabalgamientos, diapiro, modelo analógico.*

Geogaceta, 62 (2017), 19-22
ISSN (versión impresa): 0213-683X
ISSN (Internet): 2173-6545

Recepción: 31 de enero de 2017
Revisión: 15 de marzo de 2017
Aceptación: 26 de abril 2017

Introduction

The efficiency of analogue modeling in studying the progressive deformation of fold-and-thrust belts developed over incompetent *décollement* rocks has been widely proven (*e.g.* Bahroudi and Koyi, 2003; Luján *et al.,* 2003; Crespo-Blanc and Gálvez, 2008). Recently, Jiménez-Bonilla et al. (2016) modeled. Modeled progressive arcs with an indenter that increasingly protruded in map view. This backstop indented a parallelepiped made up of silicone overlaid by sand, both with constant thicknesses. Nevertheless, in natural cases the presence of diapirs is common, due to the buoyancy of salt rocks. These local heterogeneities modify drastically the 3D rheology of the sequence and consequently the nucleation of deformation structures (Roca *et al.,* 2006).

In this paper, we present the preliminary results of experiments with similar initial set up as in Jiménez-Bonilla *et al.* (2016), but with a larger parallelepiped and a slightly slower convergence velocity. It also includes small cylinders of silicone to simulate pre-deformational diapirs. Our aim is to test the influence of diapirs on the type and geometry of fold-and-thrust belt structures in progressive arcs as well as their role on the along-strike segmentation.

Model set up

Our experiments were carried out in the Analogue Modeling Laboratory of the Geodynamics Department –Earth Science Andalusian Institute in Granada. We used quartz sand (grain size between 0.2 and 0.3mm;

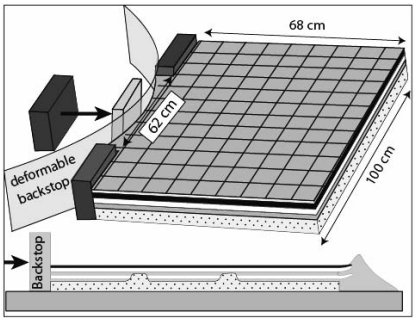

Fig. 1.- Simplified sketch of the experimental apparatus. Model set-up in oblique view and cross-section (dotted frame: silicone below the sand).

Fig. 1.- Esquema de la mesa de experimentación y del paralepípedo inicial en vista oblicua y corte (punteado: silicona debajo de la arena)

internal friction coefficient = 37.5; density = 1.77 g cm^{-3}) and silicone putty (transparent Rhodosil Gum FB of Rhone-Poulenc; density = 0.98 g cm^{-3}; viscosity=2x10^5 Pa.s). Scaling factors are the same as in Crespo-Blanc (2008). The indenter is a plastic strip pushed-from-behind in its apex by means of a screw attached to a motor drive (Fig. 1), which moved at a constant velocity (0.62 cm h^{-1}). The total displacement of the screw was around 40 cm. With progressive deformation, indenter curvature ratio diminished and its protrusion grade increased (Fig. 2; for details, see Jimenez-Bonilla *et al.*, 2016). The 100 cm x 68 cm pre-deformational package was made up of a 0.5 cm-thick silicone layer overlaid by a 1.5 cm-thick layer of sand. Two models were made with different size and number of cylinders (diapirs): three cylinders of *ca.* 10 cm of diameter in Model 1, and six cylinders with a *ca.* 4 cm diameter in Model 2. All were *ca.* 1.5 cm thick (total height) and were built just before the sieving of the sand, which freezes their shape before the deformation. Their position before deformation is drawn in figure 2. A 3-cm-side grid sieved on top of the initial parallelepiped was used as passive markers and a Mylar sheet floored the sandbox. Sand was used to confine the laterals of the models. The progressive deformation of the models was recorded by time lapse photography. In Model 2, the sand was carefully removed in order to observe the 3D-geometry of the silicone after the experiment completion.

Model results

The progressive deformation in both experiments is illustrated by the line drawings of four different deformational stages with similar apex backstop displacement (Fig. 2). Deformation was mainly accommodated by thrusts and backthrusts, favoured by the presence of a viscous substrate, coeval with strike-slip faults that formed from the very beginning of the experiments. Normal faults developed subperpendicular to thrusts at the final stages. Both models result in arcuate fold-and-thrust belts although with differences with respect to the structure distribution. Strike-slip faults acted as transfer zones bounding undeformed blocks of sand that rotated differentially, clockwise in the left part of the model and anticlockwise in the right one (in the position of Fig. 2). These vertical-axis rotations reached 40º, as shown by the grid of the most lateral blocks in A4 and B4 stages of figure 2. The arc lengthening in the deformed wedge due to the increasing protrusion of the backstop was achieved by conjugate strike-slip and normal faults.

The first structures to form were discontinuous foreland-verging thrusts and backthrusts, relayed by strike-slip faults (with a higher density in Model 1 than in Model 2). In Model 1, the nucleation of the frontal thrust of the deformed wedge seems to be associated with the diapir locations as it links those two situated to the right part of the model (A1, Fig. 2). By contrast, the influence of the small diapirs in Model 2 is not so evident and only the most frontal ones in the right part of the model are involved in the nucleation of structures (B1, Fig. 2).

When deformation proceeded, the geometry of the arcuate fold-and-thrust belt became progressively more complex. The regime of strike-slip faults may vary throughout time, as shown by the fault situated to the right part of the Model 2 (B2), which evolved into a transpression zone (B4) or by those faults in the left part of Model 1 (A3), which became transtensive. The regime variations of these faults are due to the rotation of both the structures and the blocks formed in the first stage, in turn produced by the progressive arching of the backstop.

In Model 1, silicone walls and canopies crop out at the end of the experiment (A4; Fig. 2), taking advantage of purely extensional or transtensive structures. In Model 2, the silicone reached the surface only along the lateral parts of the backstop. Another difference between both models is related to the internal deformation of individualized blocks (as shown by the grid markers): in Model 1, blocks remain relatively undeformed whereas in Model 2, internal deformation is achieved by sets of normal faults and/or thrusts, with a millimetric spacing and very small displacement (compare A4 and B4 of Fig. 2; Fig. 3A).

Figure 3B illustrates the geometry of the silicone, once sand is removed from Model 2 (compare with its final stage, B4 of Fig. 2). It clearly shows that thrusts and backsthrusts are rooted within the viscous substrate, and that strike-slip faults involve the complete vertical section. Additionally, it reveals the existence of blind thrusts (labeled b1 and b2 in figure 3B) previously covered by the frontal thrust in the right part of figure 2 (stage B4). The aforementioned millimetric spacing structures within blocks did not produce any observable deformation in the silicone layer, and are limited to the sand layer. Only two initial diapirs were preserved (circles in Fig. 3B), being the rest either covered by thrusts or drastically modified, becoming unrecognizable.

The different grade of shortening between the apex zone and the lateral parts of the progressive arc is illustrated in figures 3C and D, respectively. In the apex, a complex geometry of opposite-verging thrusts defines pop-up and pop-down structures. The high shortening in this zone produced the complete covering of a large pop-down situated on a thrust footwall (Fig. 3C). In this cross-section a vertical thickening up to 6.5 cm, that is, around 325% is observed. In other parts of the model, this thickening reached 9 cm (450%). In the right lateral part, the uppermost thrust slice is detached within the diapir (silicone underlining the uppermost thrust, Fig. 3D).

Discussion

Our experiments show that the resulting deformation style is similar to the experiments of Jimenez-Bonilla *et al.* (2016): a highly segmented, non-cylindrical arcuate fold-and-thrust belt. The resulting blocks strongly rotated clockwise or anticlockwise and are bounded by normal or strike-slip faults, which accommodated arc parallel stretching. In the model, the transfer faults, whose regime varies during progressive deformation, generated salients and recesses of the deformation front together with along-strike steep topographic variations (stages A4 and B4 of Fig. 2, Fig. 3A).

The diapirs are key heterogeneities for the nucleation and linking of structures at the beginning of the experiment. They also

facilitated the outward propagation of the deformation front when compared to a similar experiment without diapirs (see Fig. 3A-C of Jiménez-Bonilla *et al*., 2016). Then, when shortening proceeded, the diapirs were totally incorporated to the deformed wedge and transported towards the foreland through thrusting. Consequently, at late stages, their influence on the fold-and-thrust belt geometry diminished.

The nucleation of structures promoted by the presence of diapirs was also observed in the analogue models of Roca *et al.* (2006) and Rowan and Vendeville (2006). In the experiments of Crespo-Blanc and Gálvez (2008), thrusts and strike-slip faults systematically linked the diapirs. In our experiments, the large diapirs of Model 1 seem to favour the occurrence of discrete structures with centimeter-scale spacing while milimeter-scale spacing structures are more frequent in Model 2. As a consequence, Model 2 shows a more segmented fold-and-thrust belt than Model 1. This high degree of strain partitio-

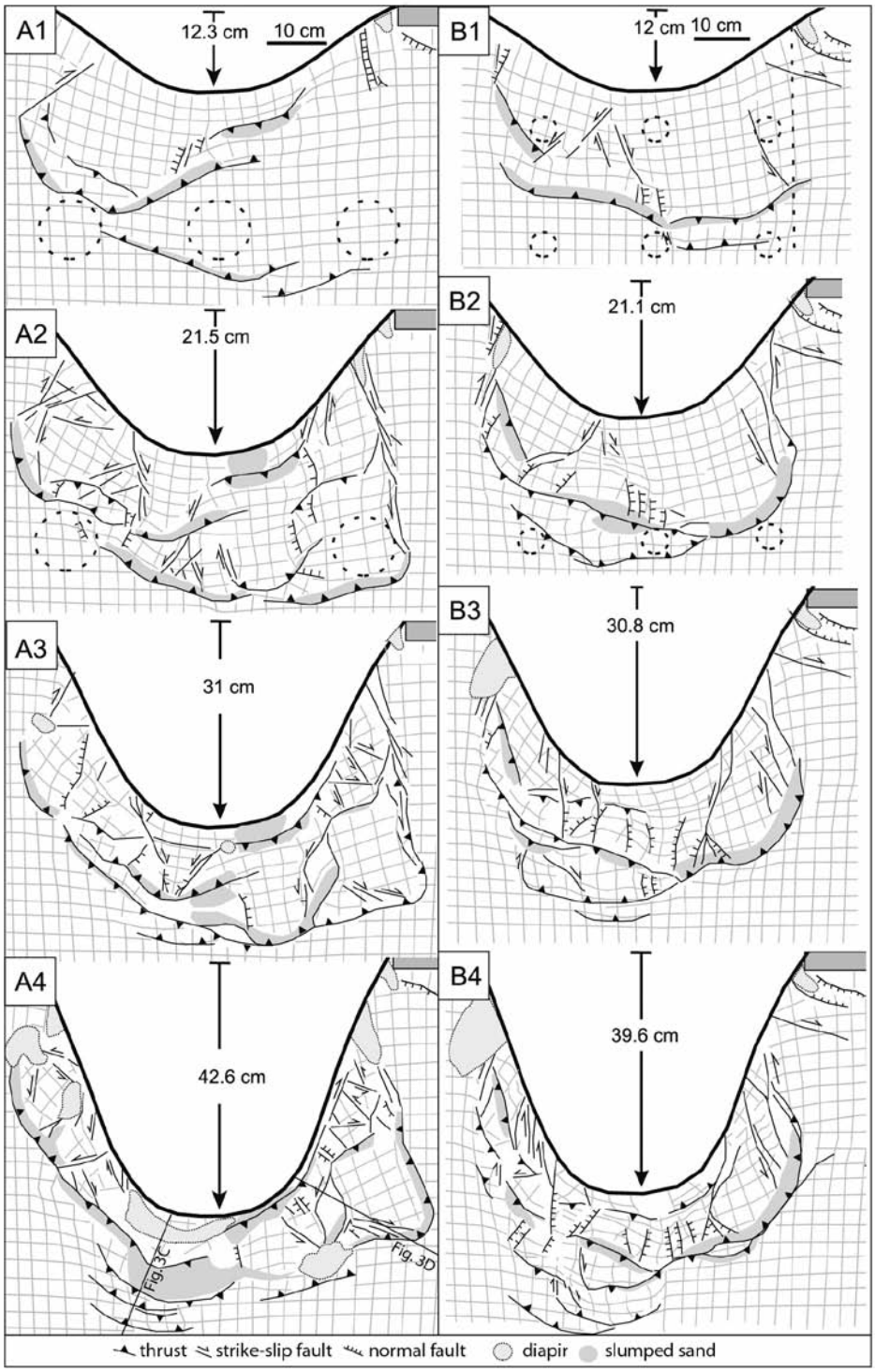

Fig. 2.- Line drawings of Model 1 (A) and 2 (B) at various deformation stages. The initial position of diapirs is marked.

Fig. 2.- Dibujos a partir de fotografías de los Modelos 1 (A) y 2 (B) en distintos estadios de deformación. La posición inicial de los diapiros está marcada.

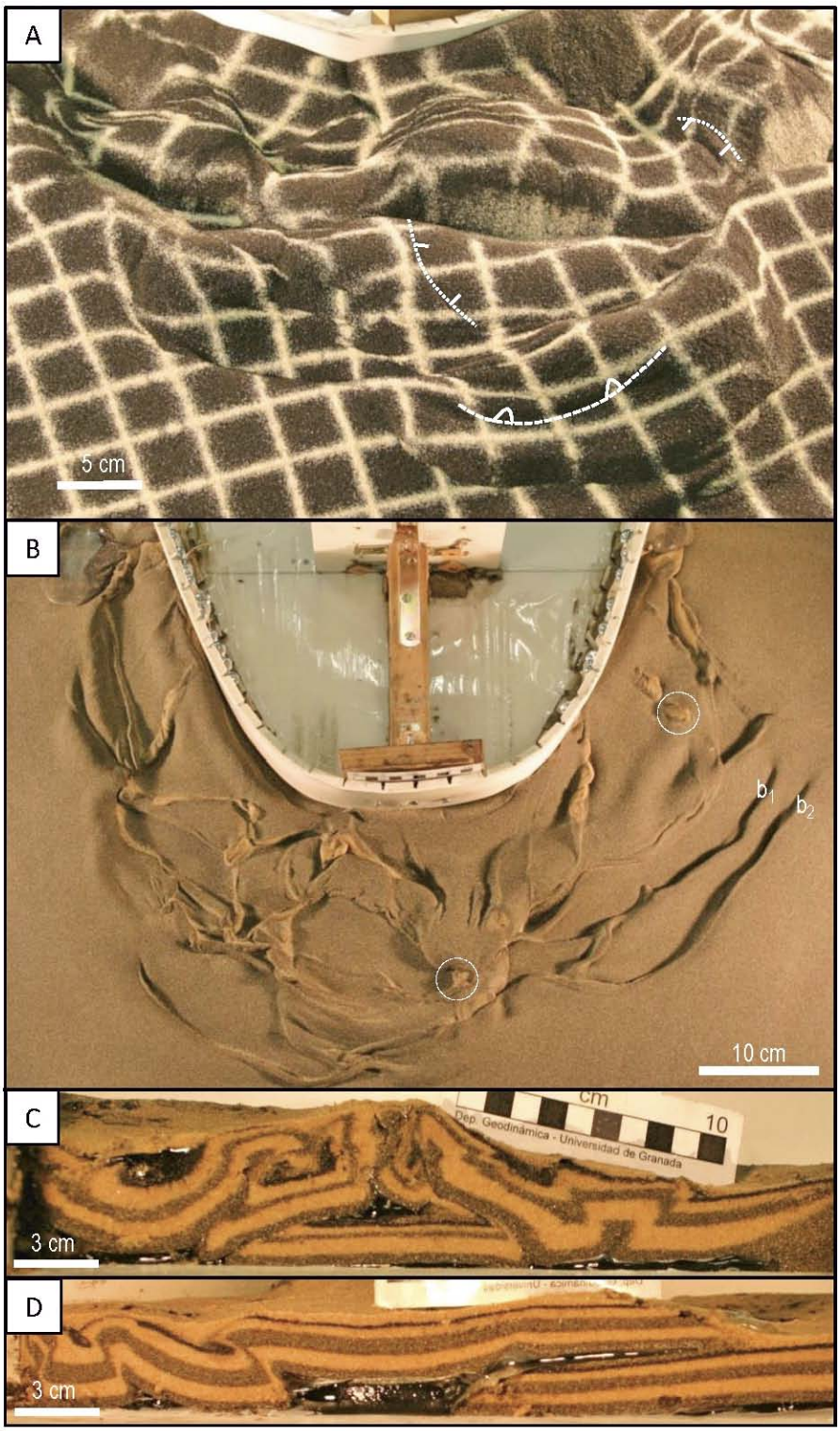

Fig. 3.- Line drawings of Model 1 (A) and 2 (B) at various deformation stages. The initial position of diapirs is marked. See color figure in the web.

Fig. 2.- Dibujos a partir de fotografías de los Modelos 1 (A) y 2 (B) en distintos estadios de deformación. La posición inicial de los diapiros está marcada. Ver figura en color en la web.

ning is the main difference with respect to the experiments without initial diapirs, as shown by the comparison of figure 3C of Jimenez-Bonilla *et al.* (2016) --with the same rheology, experimental conditions and similar movement of the backstop apex-- and that of stages A2 and B2 of figure 2 of the present paper: from the beginning of Models 1 and 2 experiments, a higher number of structures (among them, strike-slip fault systems) formed than in Jiménez-Bonilla *et al.* (2016). When shortening proceeds, shortening is mostly accommodated by the tightening of and displacement on previous structures rather than by the nucleation of new ones. It produced the thickening of the wedge. Implemented to natural cases, our results can shed light on the influence of diapirs on the strain partitioning of an arcuate, along-strike segmented fold-and-thrust belt that developed over a ductile substrate as a progressive arc.

Conclusions

1. Pre-deformational diapirs during the progressive protrusion of a backstop which curvature ratio diminished during the experiment produced a highly segmented and non-cylindrical arcuate fold-and-thrust belt.
2. Diapirs favoured the nucleation of normal and strike-slip faults, which accommodated arc-parallel stretching, and generated the individualization of blocks that rotated clockwise or anticlockwise, that is, a higher strain partitioning within the deformed wedge.
3. Large diapirs have a stronger influence on the structure nucleation than small ones. Large diapirs also favour the development of larger and wider structures; by contrast, on small diapirs, millimetric spaced structures with small displacement nucleated.

Acknowledgements

This study was supported by projects RNM-0451, CGL2013-46368-P and EST1/00231. We appreciated the reviews of E. Carola and R. Soto.

References

Bahroudi, A. and Koyi, H.A. (2003). *Journal of the Geological Society* 160(5), 719-733.

Crespo-Blanc, A. (2008). *Journal of Structural Geology* 30(1), 65-80.

Crespo-Blanc, A. and Gálvez, E. (2008). *Geogaceta* 45, 27-20.

Jiménez-Bonilla, A., Crespo-Blanc, A., Balanyá, J.C., Expósito, I. and Díaz-Azpiroz, M. (2016). *Geo-Temas* 16, CD-Rom.

Luján, M., Storti, F., Balanyá, J.C., Crespo-Blanc, A. and Rossetti, F. (2003). *Journal of Structural Geology* 25, 867–881.

Roca, E., Sans, M. and Koyi, H. (2006). *AAPG Bulletin* 90, 115–136.

Rowan, M.G. and Vendeville, B.C. (2006). *Marine and Petroleum Geology* 23, 871–891.